Astronomy & Astrophysics manuscript no. jumbos
November 15, 2023

The primoridal origin of Jupiter mass Binary Objects

Leiden Observatory, University of Leiden, Niels Bohrweg 2, 2333 CA Leiden
e-mail: hochart@mail.strw.leidenuniv.nl e-mail: spzstrw.leidenuniv.nl

Received XXXXX; accepted XXXXXX

ABSTRACT

Context. The recently observed population of 540 free-floating jupiter-mass objects, and 42 dynamically soft pairs of jupiter-mass planets, among which 2 with a tertiary companion, in the Trapezium cluster has raised interesting questions on their formation and further evolution.
Aims. We test various scenarios for the origin and survivability of these free floating jupiter-mass planets and Jupiter-mass Binary Objects (JuMBOs) in the Trapezium cluster.
Methods. The numerical calculations are performed by direct N-body integration of the stars and planets in the Trapezium cluster starting with a wide variety of planets in various configurations. We discuss four main models: $\mathcal{SPP}$ in which selected stars have two outer orbiting jupiter-mass planets; $\mathcal{SPM}$ where selected stars are orbited by jupiter-mass planet-moon pairs; $\mathcal{ISF}$ in which JuMBOs are formed in situ together with the stars. and $\mathcal{FFC}$ where we introduce a large population of free floating single jupiter-mass objects, but no binaries.
Results. Models $\mathcal{SPP}$ and $\mathcal{FFC}$ spectacularly fail to produce enough JuMBOs. Models $\mathcal{SPM}$ can produce sufficient free floaters and JuMBOs but require to start with unrealistically wide orbits for the planet-moon system around the star. The observations are best explained with in situ formation (model $\mathcal{ISF}$) of JuMBOs.
Conclusions. The observed populations of JuMBOs and free floating planets in the Trapezium cluster are best reproduced if all planets formed in pairs together with the other stars in a fractal distribution with a virial radius of ~ 0.5 pc.

Key words. ...

1. Introduction

Recently **?** reported on the discovery of 42 Jupiter-Mass Binary Objects (JuMBOs) in the direction of the Trapezium cluster. Their component masses range between 0.6 $M_{\rm Jup}$ and 14 $M_{\rm Jup}$ and have projected separations between 25 au and 380 au. Two of these objects have a nearby tertiary jupiter-mass companion. They also observed a population of 540 single objects in the same mass range. This discovery initiates the discussions on the origin and surviveability of weakly bound jupiter-mass pairs in a clustered environment.

The first single free-floating jupiter-mass objects have been found in the direction of the Trapzium cluster more than 20 years ago (**???**). Many more have been found since then, for example in the young clustered environment of Upper Scorpio (**?**), and through gravitational microlensing surveys in the direction of the Galactic bulge (**?**). Their abundance may be as high as $1.9^{+1.3}_{-0.8}$ per star (**?**), although a considerable fraction of these could be in wide orbits.

The origin of free floating planets has been actively debated. Star formation, from the collapse of a molecular cloud through gravitational instability, generally is expected to lead to objects considerably more massive than Jupiter (**??**). As a consequence, the large population of jupiter-mass free-floaters is considered to result from fully packed planetary systems, or kicked out of their orbit by encounters with other stars in the young cluster. Single jupiter-mass free floating objects then originally formed in a disk around a star but became single later in life (**??????**). The number of super-jupiter mass free floating planets formed in this way is expected to be on the order of one (~ 0.71) per star (**?**), but lower-mass free floaters orphaned this way may be much more abundant (**?**). The origin of relatively massive free-floaters through dynamical phenomena is further complicated by the tendency for lower mass planets to be more prone to ejections (**????**).

Explaining the observed abundance and mass-function of single free-floating jupiter-mass objects appears to be difficult, but recently a new population of paired free floaters have been discovered. So far, binary object have been discovered in tight (few au) orbits (**?**). Known interstellar jupiter-mass binary objects include only four objects:

- 2MASS J11193254-1137466 AB: a 5 to 10 $M_{\rm Jup}$ primary in a $a = 3.6 \pm 0.9$ au orbit (**?**).
- WISE 1828+2650: a 3 to 6$M_{\rm Jup}$ primary with a 5 $M_{\rm Jup}$ companion in an $\gtrsim 0.5$ au orbit (**?**).
- WISE J0336-014: a 8.5 to 18 $M_{\rm Jup}$ primary with a 5 to 11.5 $M_{\rm Jup}$ companion in a $0.9^{+0.05}_{-0.09}$ au orbit (**?**).
- 2MASS J0013-1143 discovered by (**?**) and suspected to be a binary by (**?**).

Such tight pairs could have formed as binary planet or a planet-moon pairs which are dislodged from their parent star to become JuMBOs (**?**). However, since only a few were discovered such an exotic scenario seems to pose a reasonable explanation for their existence. The new discovery of a rich population of 42 wide (25 au to 380 au) JuMBOs (**?**) requires a more thorough study on their origin.

Adopting a dynamical origin, or at least a dynamical history, we perform direct N-body simulations of a Trapezium-like cluster with primordial planets and JuMBOs. With the simulations, we focus on four models that could explain the abundance and orbital characteristics of the observed jupiter-mass objects (JMO) in the cluster. In this paper, we perform a rudimentary

analysis on four scenarios capable of forming JuMBOs. Alternative to forming in situ (scenario $\mathcal{ISF}$, from in-situ formation), one can naively imagine three mechanisms to form JuMBOs. (**?**) argued that these binaries could be explained from planetary systems of which the outer two planets are stripped by a passing star in a close encounter. The two ejected planets would lead to a population of free floating planets, but could also explain the observed population of JuMBOs. We call this scenario $\mathcal{SPP}$ (for star planet-planet).

Alternatively one could imagine JuMBOs to result from planet-moon pairs orbiting some star that is ejected to become a JuMBO. We call this scenario $\mathcal{SPM}$, for star planet-moon.

Finally, one could imagine that a sufficiently large population of free-floating jupiter-mass objects could lead to a population of JuMBOs by dynamical capture of one JMO by another. We call this scenario $\mathcal{FFC}$ (free floating capture). A similar scenario was proposed by (**?**) for explaining very wide stellar pairs, but the model was also adopted to account for wide planetary orbits (**??**)

We start by discussing some fundamental properties of the environmental dynamics, followed by a description of numerical simulations to characterize the parameters of the acquired JuMBOs and the resulting occurrence rates.

2. The dynamical characterization of JuMBOs

The JuMBOs discovered by (**?**) were located in the Trapezium cluster. We base our analysis on the parameters derived for this cluster by (**?**) by numerical modeling of disk-size distributions observed in the Trapezium cluster, and concluded that this distribution is best reproduced for a cluster containing ~ 2500 stars with a total mass of $\sim 900\,M_\odot$ and a half-mass radius of ~ 0.5 pc. The results were only consistent with the observations if the initial cluster density distribution represented a fractal dimension of 1.6, and was inconsistent with a (**?**) distribution. Nevertheless, for consistency with earlier studies, we perform our analysis for Plummer as well as for a fractal (with fractal dimension 1.6) distributions.

Adopting a Plummer distribution of the Trapezium cluster (with $r_{\rm vir} = 0.5$ pc virial radius), the cluster core radius $r_c \simeq 0.64 r_{\rm vir} \sim 0.32$ pc with a core mass of $250\,M_\odot$. This results in a velocity dispersion of $v_{\rm disp} \equiv GM/\sqrt{r_c^2 + r_{\rm vir}^2} \simeq 0.97$ km/s. With a mean stellar mass in the cluster core of $1\,M_\odot$ the unit of energy expressed in the kinematic temperature kT becomes $\sim 8 \cdot 10^{42}$ erg.

Jumbos are found in the mass range of about $0.6\,M_{\rm Jup}$ to $14\,M_{\rm Jup}$ and have a projected separation of 25 au and ~ 380 au. The averaged observed values are $d = 200 \pm 109$ au, $\langle M \rangle = 4.73 \pm 3.48\,M_{\rm Jup}$, and $\langle m \rangle = 2.81 \pm 2.29\,M_{\rm Jup}$. The median and 25 % to 75 % percentiles are $d = 193.75^{+78.225}_{-114.075}$ au $M = 3.67^{+1.31}_{-1.57}\,M_{\rm Jup}$, and $m = 2.10^{+1.05}_{-1.05}\,M_{\rm Jup}$.

To simplify our analysis, let us assume that the observed variation in projected distances between the two Jupiter-mass objects corresponds to an orbital separation and express distances in terms of semi-major axis (see Appendix A for motivation). In theory, the is a clear difference between the projected separation and the actual semi-major axis of the orbit, and this difference depends on the underlying eccentricity distribution (which is not measured in the observed JuMBOs), but in practice this difference is negligible compared to the 25% to 75% uncertainty intervals.

To first order, the binding energy of jumbos then ranges between $\sim 5 \cdot 10^{37}$ erg and $1.4 \cdot 10^{41}$ erg, or at most ~ 0.02 kT. This makes them soft upon an encounter with a cluster star.

The hardest JuMBO, composed of two $14\,M_{\rm Jup}$ planets in a 25 au orbit would be hard for another encountering object of less then $17\,M_{\rm Jupiter}$. For an encountering $1\,M_{\rm Jup}$ object a 25 au orbit would be hard only if the two planets are about three times as massive a Jupiter. This entails that JuMBOs are often soft for any encountering free floating planet unless they are in tight enough orbits or the perturber is of low mass. On average, soft encounters tend to soften these binaries even further (**?**), although an occasional soft encounter with another planet may actually slightly harden the JuMBO. Independent of how tight the orbit, JuMBOs are expected to be relatively short lived, because they dissociate upon a close encounter with any other cluster member. Once ionized they contribute to the population of free floating single objects. Note that in the Trapezium cluster, the orbits of 2MASS J11193254-1137466AB, WISE 1828+2650, and WISE J0336-014 would be hard; they could therefore be the fittest survivors of an underlying population.

To further understand the dynamics of the jumbos in a clustered environment, and to study the efficiency of the various formation scenarios we perform N-body calculations of the Trapezium star cluster with a population of jupiter-mass objects in various initial configurations.

3. Methodology

For each of our proposed models, $\mathcal{ISF}$ (in situ formation of jumbos), $\mathcal{SPP}$ (JuMBOs formed via ejections of a host stars outer planets), $\mathcal{SPM}$ (as planet-moon pairs orbiting a star), and $\mathcal{FFC}$ (as mutual capture of free-floaters) we perform a series of N-body simulations with properties consistent with the Trapezium cluster.

Each cluster starts with 2500 single stars taken from a broken power-law mass-function (**?**) between $0.08\,M_\odot$ and $30\,M_\odot$ distributed either in a Plummer sphere (model Pl) or a fractal distribution with a fractal dimension of 1.6 (model Fr). All models start in virial equilibrium. We run three models for each set of initial conditions, with a virial radius of 0.25 pc, 0.5 pc and 1.0 pc, called model R025, R05 and R100, respectively. We ignore stellar evolution, as well as the tidal field of the Galaxy. We further assume stellar radii to follow the zero-age main sequence, and the radius of jupiter-mass objects based on a density consistent with Jupiter.

For each of our proposed models, we initialize a population of single or binary JMO. The single (and primaries in primordial JuMBOs) are selected from a power-law mass function between $0.8\,M_{\rm Jup}$ and $14\,M_{\rm Jup}$, which is consistent with the observed mass function (**?**). We fitted a power-law to the primary-planet mass function, which has a slope of $\alpha_{\rm JuMBO} = -1.2$ (considearbly flatter than Salpter's $\alpha_{\rm Salpter} = -2.35$). The first dozen discovered free floaters already seemd to have a rather flat mass function (**?**), but the large statistics available through gravitational microlensing surveys allowd a reliable estimate of the slope, which yields $\alpha = -1.3^{+0.3}_{-0.4}$ (**?**). This mass function is somewhat steeper than the slope derived for lower-mass free floaters ($\alpha = -0.96^{+0.47}_{-0.27}$ (**?**)).

For the models with free-floating jupiter-mass objects, scenario $\mathcal{FFC}$, we sprinkle the single planets in the cluster potential as single objects using the same initial distribution function as we used for the single stars. These models were run with 1200 jupiter-mass objects (or 600 pairs), but we performed additional runs with 10^3 and 10^4 free floaters.

Primordial JuMBOs (model $\mathcal{ISF}$) are initialized with semi-major axis with a flat distribution between 10 au and 100 au (in some cases 10^4 au), an eccentricity from the thermal distribution between 0 and 1, and a mass ratio (also from the thermal distribution) between 0.2 and 1. The binary is subsequently rotated to a random orientation.

Isolated binaries, for scenario $\mathcal{ISF}$, are subsequently sprinkled in the cluster potential as single objects using the same initial distribution function as used for the single stars.

For scenario $\mathcal{SPM}$ we put the bound planet-moon pair in orbit around a star. The orbit of the planet-moon pair is circular and with a random orientation at a distance from the star such that the planet-moon's orbital separation is one-third of it's Hill radius. This guarantees a stable planet-moon pair in orbit around the selected star.

We selected the star to host such a planet-moon pair from 150 stars lower in mass than 0.6 $M_\odot$ and 150 more massive stars. The mid-mass point (of 0.6 $M_\odot$) is almost twice the mean stellar mass in the mass function.

For scenario $\mathcal{SPP}$, we select the same planet masses as for the primordial JuMBOs except that we have them orbiting one of the selected stars as a hierarchical planetary system. The distance from the first planet a_1 and the second planet a_2 (such that $a_2 > a_1$) are selected according to various criteria. The inner orbit a_1 was selected between 20 au and 2000 au from a flat distribution in a. The outer orbit, a_2, we typically chose to be ten times larger than the inner planet's Hill radius, but we also perform simulations with five times and twice the Hill radius (we call them model rH10, rH05 and rH02, respectively).

We perform an additional series of runs with pre-specified orbital separations for the two planets a_1 and a_2, to follow the model proposed in (**?**).

Each run was repeated 10 times to deal with potential statistical fluctuations, but we run 40 initiations of models $\mathcal{SPP}$_Pl_R025.

Each simulation is stopped at an age of 1 Myr, after which we study the population of free floating jupiter-mass objects and the population of JuMBOs.

To summarize, we performed the following model calculations:

$\mathcal{SPP}$	As outer orbiting planets
$\mathcal{SPM}$	As bound planet-moon pair orbiting a star
$\mathcal{FFC}$	Free floating single planets.
$\mathcal{ISF}$	In situ formation of jumbos

In figure **??** we illustrate the four models with a schematic diagram.

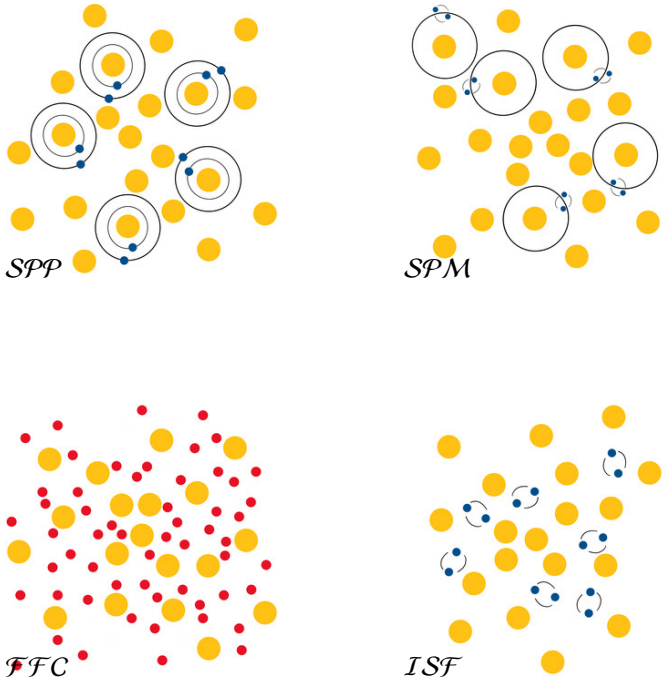

3.1. Finding JuMBOs

JuMBOs are soft in terms of the average local kinetic energy of the surrounding objects (stars and planets). This complicates the analysis of the simulation data. We genrally consider hard binary paris or multiples in direct N-body simulations are finding those soft pairs requires some extra effort.

4. Results

4.1. Model $\mathcal{SPP}$

In scenario $\mathcal{SPP}$, we follow the dynamical evolution of 1900 single stars, and 300 stars what are hosted by two planets; potentially forming 600 free-floating JMOs or 300 JuMBOs. According to (**?**), JuMBOs form naturally upon a dynamical encounter between the planetary systems and a passing star. In table 1 we summarize the results.

The $\mathcal{SPP}$ model fails to reproduce the observed population of JuMBOs by a factor of 50 to 400. The proportion of JuMBOs relative to free-floating JMO's is lower than observed values by a factor of 100. Moreover, their orbits are considerably tighter. Changing the initial distribution in semi-major axis of the inner orbit from a uniform distribution to a logarithmic distribution reduces the formation rate of JuMBOs even further.

To further explore the failure of model $\mathcal{SPP}$, we perform an additional series of simulations with pre-determined inner and outer orbital separations a_1 and a_2 using the Plummer distribution with virial radii of 0.25 pc, 0.50 pc and 1.0 pc for the stars. According to (**?**), the eventual orbital separation of the JuMBO would be consistent with the difference in orbital separation between the two planets when orbiting the star. For this reason we perform an additional series of runs with a mutual separation $a_2 - a_1 = 200$ au, expecting those to lead to consistent results in comparison with the observations. The results of these simulations are presented in figure 1.

For these models the JuMBO-formation efficiency peaks for an orbital separation $a_1 \gtrsim 1000$ au, but steeply drops for smaller values of a_1. As proposd by (**?**), we adopt a difference in the initial orbital distance of about $a_2 - a_1 = 100$ au or 200 au (see

Table 1. ...

model	n_s	$n_{(s,s)}$	$n_{(s,p)}$	n_p	$n_{(p,p)}$
$\mathcal{SPP}$_Pl_R025	2282	2	214	194	0
$\mathcal{SPP}$_Pl_R050	2219	0	281	75	0
$\mathcal{SPP}$_Pl_R100	2206	0	294	15	0
$\mathcal{SPP}$_Fr_R025	2259	96	10	494	0
$\mathcal{SPP}$_Fr_R050	2199	116	39	450	0
$\mathcal{SPP}$_Fr_R100	2229	89	64	417	0
$\mathcal{SPM}$_Pl_R025	2473	2	20	289	38
$\mathcal{SPM}$_Pl_R050	2454	0	37	147	112
$\mathcal{SPM}$_Pl_R100	2460	0	37	41	156
$\mathcal{SPM}$_Fr_R025	2337	67	16	300	73
$\mathcal{SPM}$_Fr_R050	2237	111	7	365	21
$\mathcal{SPM}$_Fr_R100	2305	84	6	336	29
$\mathcal{ISF}$_Pl_R025	2498	0	0	363	26
$\mathcal{ISF}$_Pl_R050	2498	1	0	277	59
$\mathcal{ISF}$_Pl_R100	2500	0	0	116	130
$\mathcal{ISF}$_Fr_R025	2270	43	21	279	***
$\mathcal{ISF}$_Fr_R050	2279	87	13	387	5
$\mathcal{ISF}$_Fr_R100	2273	101	5	388	6
$\mathcal{FFC}$_Pl_R025	2241	98	13	580	0.0
$\mathcal{FFC}$_Pl_R050	2274	97	6	595	0.0
$\mathcal{FFC}$_Pl_R100	2306	80	12	593	0.0
$\mathcal{FFC}$_Fr_R025	2253	103	11	584	0.0
$\mathcal{FFC}$_Fr_R050	2283	99	4	592	0.0
$\mathcal{FFC}$_Fr_R100	2259	106	10	593	0.0

Table 2. Simulation results for the models $\mathcal{SPM}$*and*FFC. The other models have an insufficently number of jumbos.

model	$\langle M \rangle$	$\langle m \rangle$	$\langle a \rangle$	$\langle e \rangle$	$\langle d \rangle$
$\mathcal{SPM}$_Pl_R025	$4.099^{+3.445}_{-2.211}$	$1.204^{+1.587}_{-0.457}$	$94.541^{+31.133}_{-35.785}$	$0.381^{+0.217}_{-0.239}$	$79.366^{+33.428}_{-37.153}$
$\mathcal{SPM}$_Pl_R050	$3.408^{+2.733}_{-1.819}$	$1.247^{+1.321}_{-0.510}$	$96.743^{+47.768}_{-36.120}$	$0.309^{+0.300}_{-0.176}$	$78.471^{+45.944}_{-35.217}$
$\mathcal{SPM}$_Pl_R100	$3.404^{+3.775}_{-1.647}$	$1.216^{+1.540}_{-0.500}$	$118.841^{+38.270}_{-42.641}$	$0.173^{+0.341}_{-0.112}$	$91.384^{+49.231}_{-34.896}$
$\mathcal{SPM}$_Fr_R025	$4.546^{+3.993}_{-2.676}$	$1.311^{+1.473}_{-0.670}$	$138.080^{+57.671}_{-64.512}$	$0.385^{+0.209}_{-0.229}$	$111.158^{+88.174}_{-60.725}$
$\mathcal{SPM}$_Fr_R050	$8.772^{+1.495}_{-5.261}$	$2.229^{+2.105}_{-1.319}$	$63.796^{+61.614}_{-6.539}$	$0.564^{+0.168}_{-0.288}$	$58.856^{+24.145}_{-20.651}$
$\mathcal{SPM}$_Fr_R100	$4.291^{+4.876}_{-2.006}$	$2.021^{+1.131}_{-1.121}$	$64.022^{+121.340}_{-18.722}$	$0.418^{+0.103}_{-0.228}$	$66.118^{+49.924}_{-29.847}$
$\mathcal{ISF}$_Pr_R025	$7.038^{+4.386}_{-4.392}$	$2.342^{+2.062}_{-1.197}$	$129.908^{+202.916}_{-56.779}$	$0.447^{+0.181}_{-0.081}$	$109.341^{+131.269}_{-53.461}$
$\mathcal{ISF}$_Pl_R050	$5.641^{+4.416}_{-2.957}$	$2.017^{+1.577}_{-0.820}$	$272.202^{+193.815}_{-146.941}$	$0.603^{+0.146}_{-0.200}$	$222.387^{+184.742}_{-112.468}$
$\mathcal{ISF}$_Pl_R100	$4.346^{+2.984}_{-2.310}$	$1.490^{+1.685}_{-0.503}$	$434.625^{+216.002}_{-254.635}$	$0.657^{+0.130}_{-0.221}$	$327.553^{+270.306}_{-184.532}$
$\mathcal{ISF}$_Fr_R025	$5.612^{+3.713}_{-3.042}$	$1.770^{+1.381}_{-0.807}$	$39.134^{+28.750}_{-13.735}$	$0.619^{+0.176}_{-0.220}$	$37.378^{+27.504}_{-19.258}$
$\mathcal{ISF}$_Fr_R050	$2.793^{+4.333}_{-1.069}$	$0.932^{+1.792}_{-0.098}$	$48.820^{+0.281}_{-22.500}$	$0.782^{+0.056}_{-0.030}$	$56.751^{+22.579}_{-30.176}$
$\mathcal{ISF}$_Fr_R100	$4.626^{+3.611}_{-1.883}$	$1.853^{+1.798}_{-0.778}$	$47.969^{+20.671}_{-24.135}$	$0.617^{+0.200}_{-0.162}$	$38.419^{+31.666}_{-20.512}$

figure 1), which would lead to JuMBO orbits in the same range. We performed a total of 45 calculations with various ranges of a_1 and a_2, of which 39 produced a total of 910 JuMBOs. The initial mean value of $a_1 - a_2 = 167 \pm 38$ au, leading to a final orbital separation of the jumbos of $a_j \sim 262 \pm 45$ au. The claim made by (**?**), that the separation distance $a_2 - a_1$ leads to JuMBOs with a similar orbital distance seems reasonable.

The rate, derived by (**?**), however, appears to be orders of magnitude smaller than they expected. They calculate the rate by means of 4-body scattering experiments, in which a star with two equal-mass planets with semi-major axes a_1 for the inner and a_2 for the other planet, encounters a single star. Their largest cross section of roughly a_1^2 is obtained if the encounter velocity $0.8 v_\star / v_1$. For an encounter at the cluster's velocity dispersion, the inner planet would then have a orbital separation of about 900 au around a 1 $M_\odot$ star.

4.2. Model $\mathcal{SPM}$

In the $\mathcal{SPM}$ models we initialize planet pairs (or planet with moons) in orbit around a star. The planet-moon system orbit was selected to mimic the observed distribution of JuMBOs and therefore are generally rather wide ($a \sim 200$ au). But we adopted relatively circular orbits ($e < 0.02$) for the planet-moon pair. To warrant stability of the star-planet-moon system, we chose an orbital separation such that the planet-moon pair stays witin 1/3th of it's Hill radius in orbit around the star. As a consequence, these systems are generally rather wide, and therefore fragile for being stripped in encounters with other stars. At the same time,

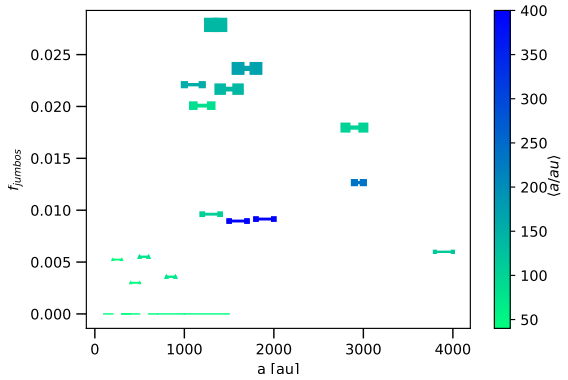

Fig. 1. The number of jumbo's produced in model $\mathcal{SPP}$, as fraction of the number of free floating planets for various simulations starting with a Plummer sphere with a virial radius of 0.5 pc. The bullet points along each line correspond with the adopted orbital separation of the two planets (a_1 and a_2). The red symbols indicate an average orbital separations for the jumbos between 25 au and 380 au. The black symbols are outside this regime. The symbol sizes give the number of jumbos (see top right for scaling) in the particular simulation.

the planet-moon pairs tend to be soft, much in the same way as the observed JuMBOs are soft. This is reflected in the rate and orbital parameters of the JuMBOs resulting from model $\mathcal{SPM}$.

In model $\mathcal{SPM}$ we find an abundance of JuMBOs with about 500 per cluster when we start with a Plummer distribution, and about 100 for the fractal models (starting with 600 pairs). The lower frequency for the fractal models reflects the more dynamic environment in which JuMBOs are easily ionized. This trend is also noticeable in the number of stellar binaries and free floating planets, but also in the JuMBO orbital parameters. JuMBOs originating from the Plummer models tend to be rather circular and somewhat wider than those surviving in the fractal model. These trends are indepenedend of the cluster density (or virial radius). We do expect some difference in the JuMBO population as a fuction of the initial cluster density, but the distribution JuMBO parameters in the simulations are wide and they probaby do not form the right population to make such a distinction.

4.3. Model $\mathcal{FFC}$

4.4. Model $\mathcal{ISF}$

4.5. stellar and planetary collisions

No collisions occur between stars or planets in a Plummer models, where in the fractal models collisions these events become rather common.

in the $\mathcal{SPM}$ models 12.9 ± 8.0 stars experienced a collision with another star. No planets collided with other planets, or with a star.

5. Discussion

(**?**) argued that JuMBOs potentially originate from tilted circumbinary planets. Formed as a –sort-of– planet-moon system in a wide orbit around a star, that is strippied from the host star by the cluster potential or a relatively wide encounter with another star.

Single free floating planetary objects were discovered in abundance (between 70 and 170 candidates) before in the Upper

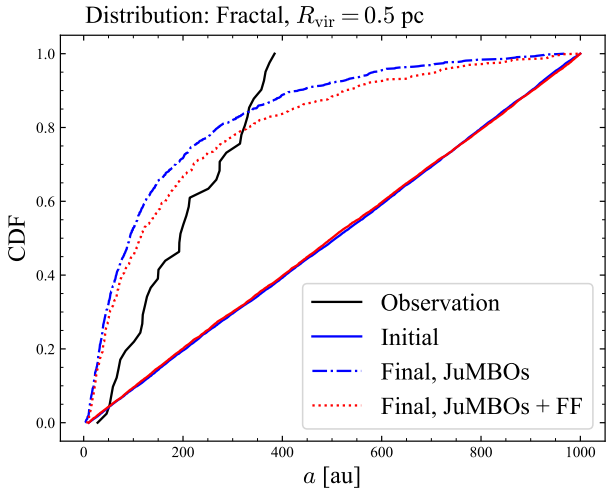

Fig. 2.

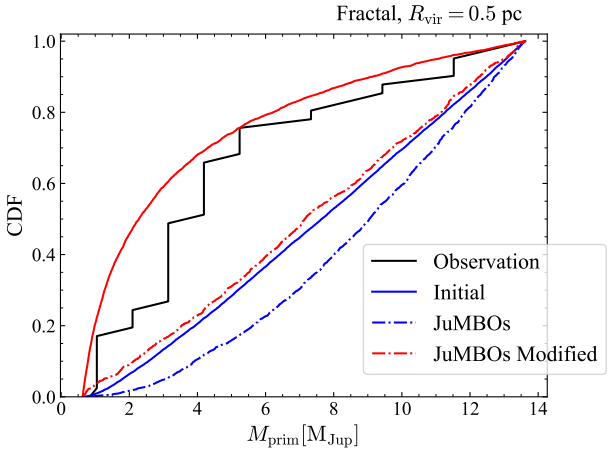

Fig. 3.

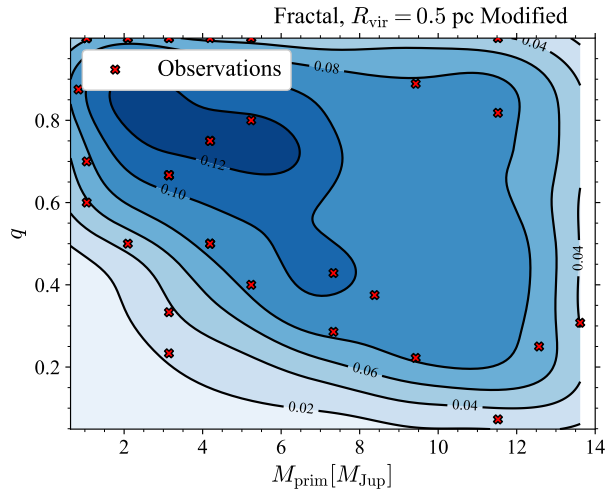

Fig. 4.

Scorpius association (**?**), but these were considered to be single free floaters. With an age of about 11 Myr (**?**), Upper Scorpio is expected to be rich in single jupiter mass free floating planets, but binaries will be rare as these have been broken.

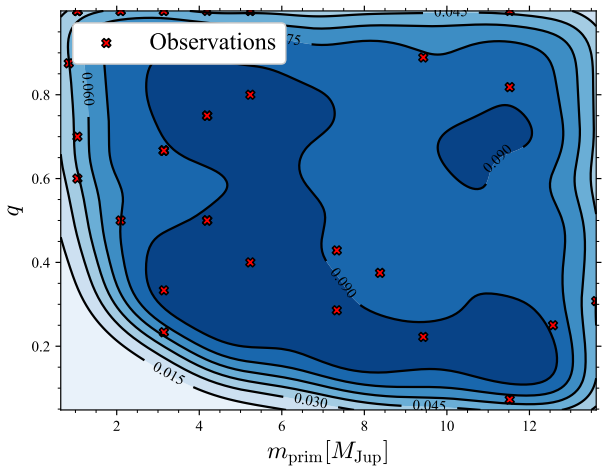

Fig. 5.

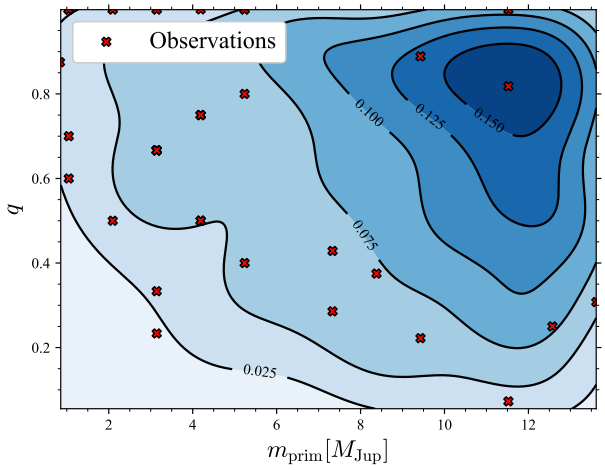

Fig. 6.

The orbital parameters of the JuMBOs hardly seem to depend on the cluster density (or virial radius). We do expect some difference in the JuMBO population as a fuction of the initial cluster density, but the distribution JuMBO parameters are wide and they probaby do not form the right population to make such a distinction.

5.1. The failure of model $\mathcal{SPP}$

Note that an inner orbital separation of $a_1 = 800$ au for a 10 $M_{\rm Jup}$ planet leads to a Hill radius of about 150 au. An orbit with $a_2 = 1000$ au, is probably only marginally stable. Still, even in those runs the total number of JuMBOs remains small compared to the number of free floaters.

In (**?**), the highest cross section is achieved for the orbital velocity of the inner-most planet as fraction of the typical encounter velocity $v1/v_{\rm disp} \sim 0.8$. With a cluster velocity dispersion of ~ 0.8 km/s, the orbital velocity roughly 1 km/s. Around an 1 $M_\odot$ star such a velocity is obtained, assuming a Kepler orbit, at an orbital separation of 800 au. It turns out, that the results of the cross section calculations performed by (**?**) are consistent with our direct N-body simulation, but that the adopted initial orbital separation is too wide in comparison with a realistically population of inner planetary orbits for jupiter-mass planets. Observational selection effect in finding $\gtrsim 800$ au jupiter-mass planets are quite severe, but we consider it unrealistic to have 600 out of 2500 stars to be orbited by such wide planetary systems. In particular, when one considers the small sizes of the observed disks in the Trapezium cluster, which today are all smaller than 400 au (**?**).

5.2. JuMBOs as former planet-moon pairs, model SPM

5.3. JuMBOs as former multi-planet systems, model SPP

According to (**?**), jumbos form naturally upon a dynamical encounter between two stars one of which with orbited by a binary planet or planet-moon system.

Both calculations (**?**) and (**?**) adopt scattering experiments to determine the formation rate of jumbos from their adopted initial conditions.

5.4. JuMBOs formed for capture of free-floating planets, model FFC

5.5. JuMBOs as primoridal low-mass object pairs, model SPP

Recently 70 to 170 candidates) before in the 10 Myr old association Upper Scorpius (**?**), but these were considered to be single.

5.5.1. Further constraining the initial conditions

Using the results of the general models, we alter our initial conditions with the aim of mimicking observations. Doing so allows us to disentangle aspects of the cluster history, allowing for predictions on the properties of JuMBO formation. These runs correspond to the middle segment of table 6.

For all models, we constrain $N_{\rm JuMBO} + N_{\rm FF}$ to values reflecting the total planetary-mass population observed in **?**, keeping in mind the survival rate of JuMBO systems based on previous results to decide on the initial value of $N_{\rm JuMBO}$. The range of mass ratio and mass value remains unchanged. However, now the mass ratio follows a thermal distribution to reflect the abundance of $q = 1$ observations, whilst the mass of the objects follows a power-law distribution with $\alpha = -1.2$. The semi-major axis is uniformly distributed between the restricted range $a \in [25, 100]$ au. Here, the lower bound reflects the restrictions of observational resolution in the original study (**?**).

Models 'F050C' and 'F0FFOC' look at scenarios where the initial JuMBO population has an eccentricity ranging between $e \in [0, 0.2]$ sampled from a uniform distribution. For all other models, the eccentricity remains thermalised and ranges between $e \in [0, 0.9]$.

6. Conclusion

The discovery of relatively wide pairs of jupiter-mass planetary objects in the Trapezium cluster emphasizes our limited understanding of low-mass star and planet formation. In order to derive characteristcs for their origin we performed simulations of Trapezium-equivalent stellar clusters (2500 stars with a virialized ~ 0.5 pc radius) with various compositions of planetary objects and stars.

Models in which planets form in wide circum-stellar orbits, as proposed by (**?**), produce many single free floating planets, but an insufficient number of planet pairs per cluster. The ratio of single to pairs of planets is too low by a factor of 60 to 400.

Table 3. Initial conditions of the various configurations. The nomenclature is as follows: The first letter identifies the cluster distribution. The number denotes the initial virial radius, 'FF' denotes the presence of Jupiter-mass free floaters, 'x' whether the system contains an abundance (excessive/extra) amount of these free floaters, 'O' denotes systems whose JuMBOs have their initial parameters constrained by the observational data and finally 'C', systems whose initialised JuMBOs are on circular orbits. Column 1: The model used. Column 2: The number of simulations for the given configuration. Column 3: The initial virial radius of the system. Column 4: The number of initialised JuMBOs. Column 5: The number of initialised free floaters.

Model	$N_{\rm runs}$	$R_{\rm vir}$ [pc]	$N_{\rm JuMBO}$	$N_{\rm FF}$
F05	20	0.5	500	0
F05FF	20	0.5	500	500
F1	20	1.0	500	0
P05	20	0.5	500	0
P05FF	20	0.5	500	500
P1	20	1.0	500	0
F05O	10	0.5	275	0
F05FFO	10	0.5	170	400
F05OC	10	0.5	275	0
F05FFOC	10	0.5	170	400
P05FFO	10	0.5	60	500
F05FFxJ	5	0.5	500	10^4
F05FFx	5	0.5	0	10^4

The models in which pairs of planetary-mass objects orbit stars in the form of a planet-moon system, produce many free floating planetary pairs, and in the proper range of orbits. In particular the models that start with fractal initial conditions tend to produce a fraction of jumbos of among free floating planets $O(0.1)$, which is close to the observed value of 0.078 ± 0.012. The absolute numbers are a bit high though, by a factor of two, but that is easily solved by starting with fewer systems. Although the distribution in orbital separation matches the observations by constructing the initial conditions appropriately, these models prediction rather low-eccentricities ($e \lesssim 0.4$).

For the model to produce a sufficient number of JuMBOs it requires planet-moon pairs form in $\gtrsim 1000$ au orbits around their parent star. Such wide orbits are exotic considering the fact that the circum-stellar disks observed in the Trapezium cluster tend to be smaller than 400 au. We therefore do not see how such wide planet-moon pairs can form around stars.

Starting with a enormous population of ($\gtrsim 10^4$) isolated free-floating planetary mass objects among the stars would grossly overproduce the expected number of free floaters, which is not observed, and still fails to reproduce the observed number of JuMBOs. This model, however, naturally leads to a mass-ratio distribution skewed to unity, as is observed. We consider this model undesireable by the lack of a large ($\gtrsim 10^4$) population of free floating planets in the Trapezium cluster.

Ruling out models $\mathcal{SPP}$, $\mathcal{SPM}$ and $\mathcal{FFC}$, we are left with the simplest and most satisfactory solution in which JuMBOs form together with the single stars in the cluster. This model does not only reproduce the observed rates, it can subsequently also be used to further constrain the initial conditions of JuMBOs.

In the Plummer models, 80% of JuMBOs are ionized within 1 Myr. The observed population of free floaters and JuMBOs can then be reproduced if the cluster was born with some 500 free floating jupiter-mass planets and $\sim$ 50 JuMBOs. The current observed primary and secondary masses of JuMBOs would then still reflect the conditions at birth, but the semi-major axis and eccentricity distributions would have been affected by encounters with other cluster members. These processes tend to drive the eccentricity distribution to resemble the thermal distribution (probably with an excess of high ($\gtrsim 0.8$) eccentricities (**?**). The semi-major axes of the jumbos would have widened, on average by approximately 5% due to encounters with other cluster members (mainly stars and free-floating planets).

Alternative to a Plummer initial stellar distribution we experimented with fractal distributions, which also satisfactorily reproduces the observed populations. In the fractal models, $\sim 90\,\%$ of the priordial JuMBOs become ionized, and in principle the entire observed populations of free-floating jupiter mass objects and JuMBOs can be explained by a single population of primordial JuMBOs. We then conclude that single jupiter mass objects are preferentially born in pars with a rather flat distribution in orbital separations with a maximum of about 100 au or 200 au.

This model satisfactorily explains the observed orbital separation distribution, with a $\sim$ 15% excess of systems with a separation $\gtrsim 400$ au. We do expect a rich population of orbits with separation smaller than the observed 25 au, possibly down to sub-au scales. The masses of the primaries in the planet pairs, and the mass-ratio distribution are then hardly affected by the past $\sim$ 1 Myr evolution of the Trapezium cluster.

We have a slight preference for the $\mathcal{ISF}$ fractal models with 0.5 pc virial radius because hierarchical triple planets form naturally in roughly the observed proportion (on average 4 triples among $\sim$ 40 pairs and $\sim$ 500 single planets). The singles then originate from broken up pairs, and the trples form in interactions between two planet pairs. The dynamical formation of soft triple planets is quite remarkable, and observational follow-up would be of considerable interest.

We conclude that the observed JuMBOs in the Trapezium cluster formed as planetary pairs together with the other stars.

6.1. $\mathcal{FFC}$: Free Floating Jupiter Mass Objects

In our final scenario, $\mathcal{FFC}$, we scatter 10^4 Jupiter-mass objects in the cluster with no JuMBO systems initialised. The main aim is to see the efficiency of forming JuMBOs via mutual captures of free floaters. The parameters of the cluster and free floaters remain unchanged to those listed in section **??**.

7. Results

7.1. $\mathcal{ISF}$

In figure 7 we illustrate how the fraction of jumbos decreases with time.

Figure 8 shows the final snapshot of a F05 simulation. It represents the typical final state of simulations evolved during our $\mathcal{ISF}$ and $\mathcal{FFC}$ runs. The density map reveals the final positions of all objects simulated. Surviving JuMBOs are scattered onto the plot with red outlines. Overlayed are also the positions of known stars (in yellow) taken from **??** and the positions of known JuMBOs (black outlined points) (**?**).

Table 7 summarises all our final results. We begin our discussion on the $\mathcal{ISF}$ models by looking at the general models (top segment of table 6).

7.1.1. Open Parameter Space

Overall, JuMBOs are more likely to survive in a Plummer-like cluster. Their survival rates increase by a factor of $\sim$ 18 compared with likewise configurations initialised under a Fractal dis-

Table 4. ...

model	a_2/au	$n_{(s,s)}$	$n_{(s,p)}$	n_p	$n_{(p,p)}$			
$\mathcal{ISF}$_Fr_R05	50	83.0	11.0	531.0	29.0	0	0	0
$\mathcal{ISF}$_Fr_R05	100	102.0	11.0	141.0	24.0	0	0	0
$\mathcal{ISF}$_Fr_R05	150	70.0	10.0	562.0	14.0	0	0	0
$\mathcal{ISF}$_Fr_R05	200	79.0	7.0	565.0	14.0	0	0	0
$\mathcal{ISF}$_Fr_R05	300	88.0	6.0	578.0	8.0	0	0	0
$\mathcal{ISF}$_Fr_R05	400	102.0	15.0	579.0	3.0	0	0	0
$\mathcal{ISF}$_Fr_R05	800	80.0	17.0	579.0	2.0	0	0	0
$\mathcal{ISF}$_Fr_R05	1600	86.0	10.0	588.0	1.0	0	0	0

Table 5. ...

model	a/au	$\langle M \rangle$	$\langle m \rangle$	$\langle a \rangle$	$\langle e \rangle$	$\langle d \rangle$
$\mathcal{ISF}$_Fr_R05	50	$3.713^{+3.427}_{-1.494}$	$0.731^{+0.405}_{-0.440}$	$39.002^{+7.422}_{-5.958}$	$0.502^{+0.228}_{-0.213}$	$33.830^{+12.064}_{-10.795}$
$\mathcal{ISF}$_Fr_R05	100	$6.032^{+2.538}_{-3.590}$	$1.301^{+1.066}_{-0.679}$	$47.183^{+17.561}_{-18.831}$	$0.525^{+0.242}_{-0.225}$	$36.550^{+19.469}_{-16.452}$
$\mathcal{ISF}$_Fr_R05	150	$4.037^{+5.264}_{-1.552}$	$0.638^{+1.067}_{-0.255}$	$41.691^{+106.367}_{-9.897}$	$0.700^{+0.166}_{-0.131}$	$53.255^{+40.398}_{-17.021}$
$\mathcal{ISF}$_Fr_R05	200	$4.223^{+1.716}_{-1.225}$	$0.877^{+1.571}_{-0.463}$	$43.394^{+23.126}_{-16.220}$	$0.688^{+0.093}_{-0.336}$	$39.605^{+40.066}_{-17.487}$
$\mathcal{ISF}$_Fr_R05	300	$5.278^{+3.788}_{-2.439}$	$1.291^{+1.537}_{-0.341}$	$36.812^{+11.837}_{-7.330}$	$0.573^{+0.239}_{-0.179}$	$46.200^{+7.743}_{-20.497}$
$\mathcal{ISF}$_Fr_R05	400	$3.332^{+6.031}_{-0.668}$	$0.763^{+1.262}_{-0.285}$	$37.815^{+62.038}_{-5.966}$	$0.280^{+0.176}_{-0.077}$	$40.852^{+81.719}_{-4.104}$
$\mathcal{ISF}$_Fr_R05	800	$3.247^{+0.940}_{-0.940}$	$0.388^{+0.080}_{-0.080}$	$25.646^{+0.708}_{-0.708}$	$0.480^{+0.019}_{-0.019}$	$20.344^{+10.236}_{-2.360}$
$\mathcal{ISF}$_Fr_R05	1600	$2.315^{+0.000}_{-0.000}$	$0.056^{+0.000}_{-0.000}$	$25.652^{+0.000}_{-0.000}$	$0.116^{+0.000}_{-0.000}$	$20.912^{+1.166}_{-0.780}$

Table 6. Initial conditions of the various configurations. The nomenclature is as follows: The first letter identifies the cluster distribution. The number denotes the initial virial radius, 'FF' denotes the presence of Jupiter-mass free floaters, 'x' whether the system contains an abundance (excessive/extra) amount of these free floaters, 'O' denotes systems whose JuMBOs have their initial parameters constrained by the observational data and finally 'C', systems whose initialised JuMBOs are on circular orbits. Col. 1: The model used. Col. 2: The number of simulations for the given configuration. Col. 3: The initial virial radius of the system. Col. 4: The number of initialised JuMBOs. Col. 5: The number of initialised free floaters.

Model	$N_{\rm runs}$	$R_{\rm vir}$ [pc]	$N_{\rm JuMBO}$	$N_{\rm FF}$
F05	20	0.5	500	0
F05FF	20	0.5	500	500
F1	20	1.0	500	0
F05FFL	5	0.5	500	500
P05	20	0.5	500	0
P05FF	20	0.5	500	500
P1	20	1.0	500	0
F05O	10	0.5	270	0
F05FFO	10	0.5	200	140
F05OC	10	0.5	270	0
P05FFO	10	0.5	70	400

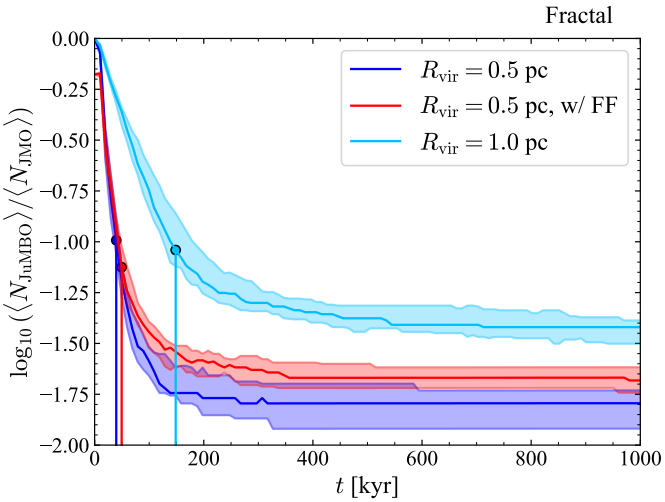

Fig. 7.

tribution. Even so, no configuration is successful in reproducing the 9% fraction of JuMBOs relative to free-floaters observed. Instead, in the $\mathcal{ISF}$ scenarios, the fraction of JuMBOs to JMO free floaters ranges between 0.29 ∼ 1.3 for Plummer runs and 0.01 ∼ 0.02 for Fractals.

The increase of JuMBO surviveability in runs including free-floaters could be due to the rare JMO-JuMBO interaction hardening the binary, also resulting in a decrease in its gravitational cross section. We believe this to be the case even though as discussed in the introduction JuMBOs will tend to ionise, even when interacting with other JMO, since, although increasing the number of JMOs enhances the chances of two free-floaters (or a free floater and ionised JMO) settling into a newly formed binary, on average, only 0.4 new JuMBO systems emerge per run for F05 runs compared to the 0.65 in F05FF (from 1.75 to 3.15 between P05 and P05FF).

Figures 9 show the cumulative distribution function (CDF) for the semi-major axis of surviving JuMBOs during F05, F05FF and F1 runs. The Fractal distribution efficiently prunes off any wide orbits since its violent nature provokes many encounters result in the ionisation of JuMBO systems, moreso the ones on wide orbits who have a larger cross-section. The tendency for JuMBOs to ionise at any encounter is reflected by the little variation between runs of the same virial radius. We also note the tendency for JuMBOs to ionise even when a JMO perturbs the system as reflected with the decrease in median semi-major axis between models P05 and P05FF from $\langle a \rangle \sim 268$ au to $\langle a \rangle \sim 187$ au.

Table 7. Statistics on the surviving JuMBOs. ⟨...⟩ gives the median, while the ± denote where the lower and upper quartile lie. Col. 1: The fraction of JuMBOs present at the end of the simulation relative to the number initialised. Col. 2: The fraction of JuMBOs with projected separation, $r_{ij} > 25$ au. Col. 3: The mass ratio of JuMBO systems. Col. 4: The primary mass of the JuMBO system. Col. 5: The semi-major axis of the JuMBO system. Col. 6: The eccentricity of the system.

Model	$f_{\rm surv}$	$f_{r_{ij}\geq 25{\rm au}}$	$\langle q\rangle$	$\langle M_{\rm prim}\rangle$ [$M_{\rm Jup}$]	$\langle M_{\rm sec}\rangle$ [$M_{\rm Jup}$]	r_{ij} [au]	$\langle a\rangle$ [au]	$\langle e\rangle$
F05	$0.02^{+0.00}_{-0.00}$	$0.67^{+0.19}_{-0.07}$	$0.61^{+0.21}_{-0.24}$	$8.6^{+2.4}_{-3.3}$	$4.2^{+3.2}_{-1.9}$	38^{+52}_{-18}	39^{+50}_{-16}	$0.67^{+0.16}_{-0.19}$
F05FF	$0.04^{+0.00}_{-0.01}$	$0.61^{+0.02}_{-0.11}$	$0.54^{+0.24}_{-0.24}$	$8.8^{+2.7}_{-2.6}$	$3.9^{+2.5}_{-2.0}$	30^{+43}_{-16}	37^{+41}_{-20}	$0.62^{+0.14}_{-0.21}$
F1	$0.04^{+0.00}_{-0.01}$	$0.72^{+0.11}_{-0.06}$	$0.60^{+0.20}_{-0.24}$	$8.3^{+2.4}_{-3.0}$	$3.8^{+2.4}_{-1.9}$	64^{+98}_{-40}	67^{+83}_{-38}	$0.68^{+0.16}_{-0.19}$
F05FFL	$0.03^{+0.00}_{-0.00}$	$0.46^{+0.07}_{-0.07}$	$0.57^{+0.31}_{-0.25}$	$8.1^{+2.9}_{-2.7}$	$2.7^{+3.1}_{-1.0}$	33^{+20}_{-18}	20^{+15}_{-9}	$0.61^{+0.20}_{-0.19}$
P05	$0.37^{+0.01}_{-0.02}$	$0.94^{+0.02}_{-0.01}$	$0.55^{+0.23}_{-0.23}$	$8.3^{+2.7}_{-3.1}$	$3.6^{+2.7}_{-1.8}$	233^{+234}_{-137}	268^{+237}_{-152}	$0.68^{+0.16}_{-0.22}$
P05FF	$0.52^{+0.02}_{-0.00}$	$0.92^{+0.00}_{-0.01}$	$0.57^{+0.21}_{-0.24}$	$8.1^{+2.8}_{-3.2}$	$3.4^{+2.7}_{-1.7}$	162^{+167}_{-94}	187^{+176}_{-106}	$0.61^{+0.14}_{-0.18}$
P1	$0.72^{+0.02}_{-0.01}$	$0.97^{+0.00}_{-0.01}$	$0.54^{+0.24}_{-0.23}$	$7.8^{+3.0}_{-3.0}$	$3.3^{+2.5}_{-1.6}$	344^{+271}_{-188}	396^{+250}_{-206}	$0.68^{+0.16}_{-0.20}$
F05O	$0.02^{+0.00}_{-0.01}$	$1.00^{+0.00}_{-0.16}$	$0.81^{+0.09}_{-0.17}$	$4.0^{+2.6}_{-1.9}$	$2.8^{+1.7}_{-1.5}$	61^{+46}_{-24}	67^{+48}_{-22}	$0.67^{+0.14}_{-0.19}$
F05FFO	$0.03^{+0.00}_{-0.00}$	$0.8^{+0.02}_{-0.15}$	$0.76^{+0.10}_{-0.17}$	$3.4^{+3.4}_{-1.7}$	$1.8^{+2.0}_{-0.8}$	44^{+37}_{-18}	46^{+38}_{-22}	$0.69^{+0.15}_{-0.18}$
F05OC	$0.02^{+0.01}_{-0.00}$	$0.67^{+0.19}_{-0.07}$	$0.81^{+0.10}_{-0.14}$	$4.7^{+3.2}_{-2.7}$	$3.6^{+2.6}_{-2.02}$	46^{+36}_{-26}	49^{+28}_{-28}	$0.45^{+0.33}_{-0.23}$
P05FFO	$0.76^{+0.01}_{-0.01}$	$0.89^{+0.03}_{-0.03}$	$0.78^{+0.12}_{-0.15}$	$3.7^{+3.5}_{-2.1}$	$2.1^{+2.5}_{-1.2}$	90^{+86}_{-44}	105^{+86}_{-47}	$0.61^{+0.15}_{-0.17}$

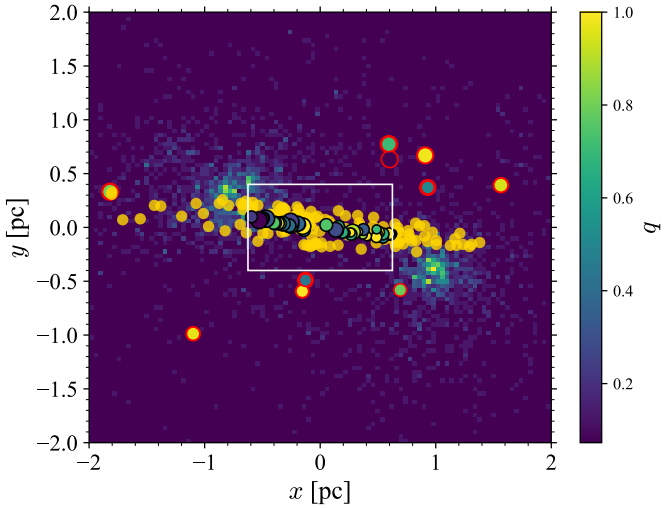

Fig. 8. Schematic of a F05 simulation. The density map denotes final positions of simulated objects, the translucent yellow points observed stars taken from **??**. The white frame denotes the observed region in **?**, with black outlined dots denoting observed JuMBOs. Red outlined dots denote the final JuMBOs observed in our simulation.

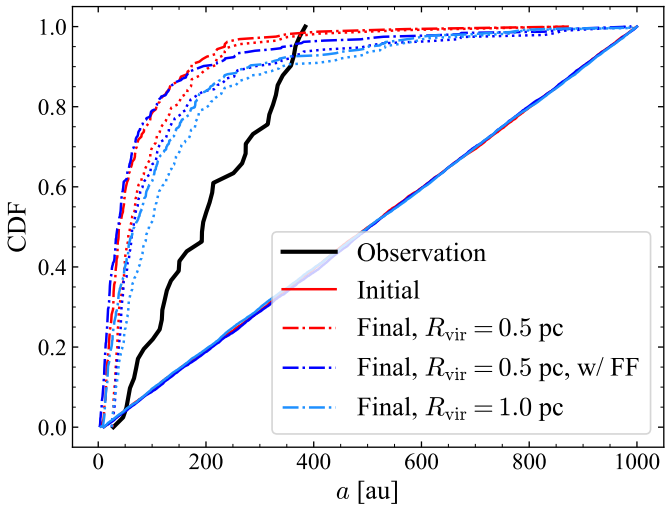

Fig. 9. CDF of surviving JuMBO semi-major axis distribution for models F05, F05FF, F1. Dash-dotted curves incorporate all JuMBO systems, whereas dotted ones only those with a projected separation exceeding 25 au.

The results in semi-major axis' during the Fractal runs are much smaller than those observed, suggesting the $\mathcal{ISF}$ model fails to capture the birth of such environments. Contrariwise, and as seen in figure 10, Plummer models are capable of preserving the wider orbits. This, however, is due to the environment to output similar values to those inputted since it is less violent by nature.

Indeed, keeping in mind that our JuMBOs in these models are initialised with a uniform mass distribution, we see the uniformity reflected in the final $M_{\rm prim}$ vs. q parameter space shown in figure 11. Although it also fails at reproducing observations, figure 12 shows more structure and less uniformity in the distribution of JuMBOs in ($M_{\rm prim}$, q)-space as reflected by the starker contrasts between contour levels and smaller high-density regions.

Given this, although a correct calibration of initial conditions during Plummer runs will give back JuMBOs with similar properties to those observed, the extent of fine tuning needed and lack of natural mechanism to remove the tail end of wide-orbit JuMBOs, we can apply Occam's razor to rule it out as an initial conditions.

The omission of Plummer models is further supported since no systems formed dynamically during the runs. This contradicts with the observed presence of two triple JMO systems. Given this, we restrict ourselves to Fractal models as we believe this better represents the Trapezium cluster, a fact agreeing with **?**.

7.1.2. Evolving till 10 Myr: TO CHECK – STILL IN RUNS

Here we analyse results for a system evolved to 10 Myr, with the aim of looking at the survival of JuMBOs in more estab-

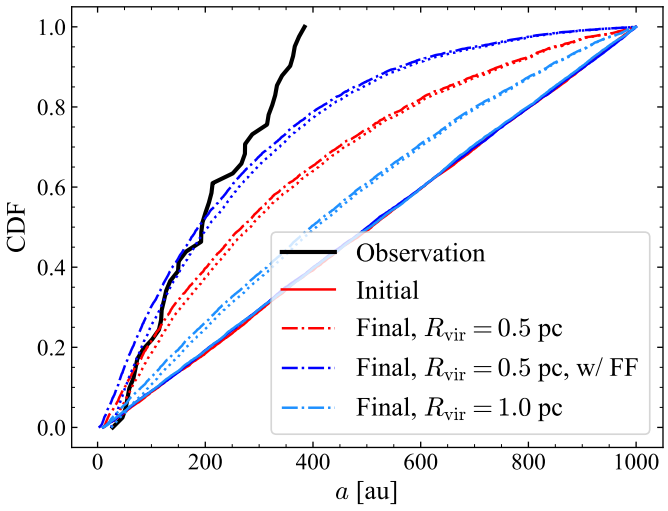

Fig. 10. CDF of surviving JuMBO semi-major axis distribution for models P05, P05FF, P1. Dash-dotted curves incorporate all JuMBO systems, whereas dotted ones only those with a projected separation exceeding 25 au.

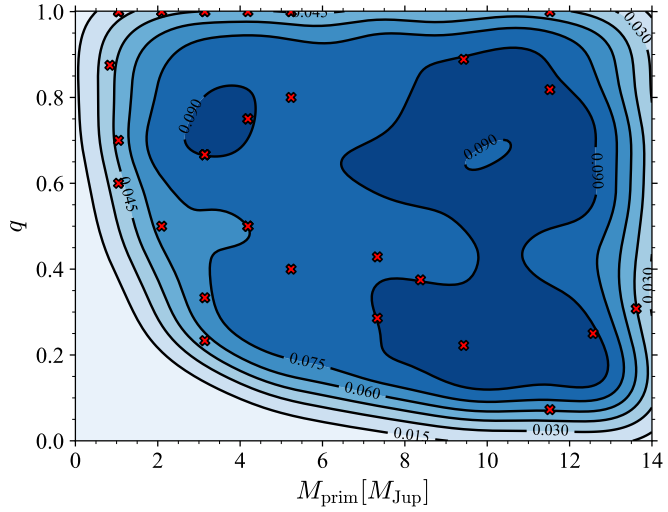

Fig. 11. Contour plot of $M_{\rm prim}$ vs. q for model P05FF. Red crosses denote where observed JuMBOs lie.

lished systems. Overall, the JuMBO survival rate decreases and the ones surviving exhibit tighter orbits with $\langle a \rangle \sim 20$, a regime in which two 3 $M_{\rm Jup}$ systems become hard for $\sim M_{\rm Jup}$ interactions.

Figure 13 shows the distribution of $M_{\rm prim}$ of surviving JuMBOs. The little difference observed between F05FF and F05FFL is reflected by the similarities between their median and interquartile (IQR) range ($\langle M_{\rm prim} \rangle \sim 8.8$ and $\langle M_{\rm prim} \rangle \sim 8.1$ for F05FF and F05FFL respectively). The fact that this holds for all configurations simulated implies the ease at which JuMBO systems ionise upon interaction.

Figure 14 shows the contour plot of $M_{\rm prim}$ vs. q. As before, the parameter space poorly replicates the observed distribution with most of the JuMBOs having too large a primary mass. We keep this in mind for simulations in the following subsection where we initialise JuMBOs with a power-law of $\alpha = -1.2$, the power-law found to best fit observations.

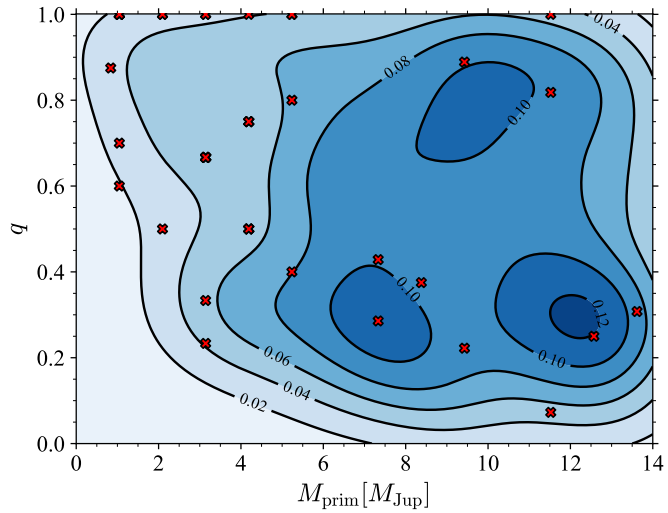

Fig. 12. Contour plot of $M_{\rm prim}$ vs. q for model F05FF. Red crosses denote where observed JuMBOs lie.

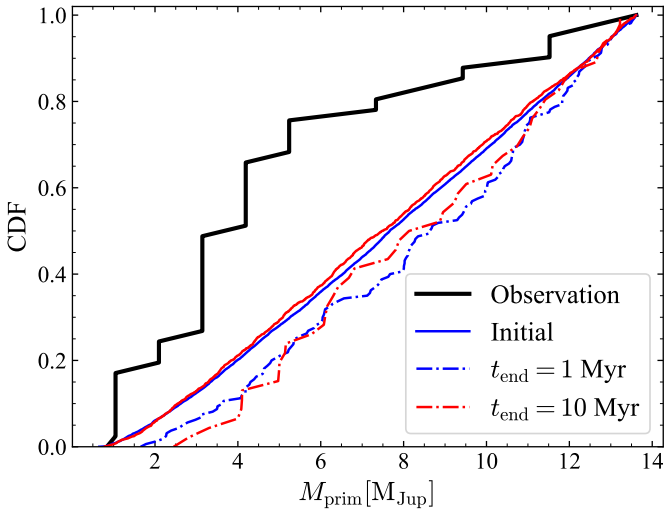

Fig. 13. CDF of surviving JuMBO $M_{\rm prim}$ for models F05FF and F05FFL.

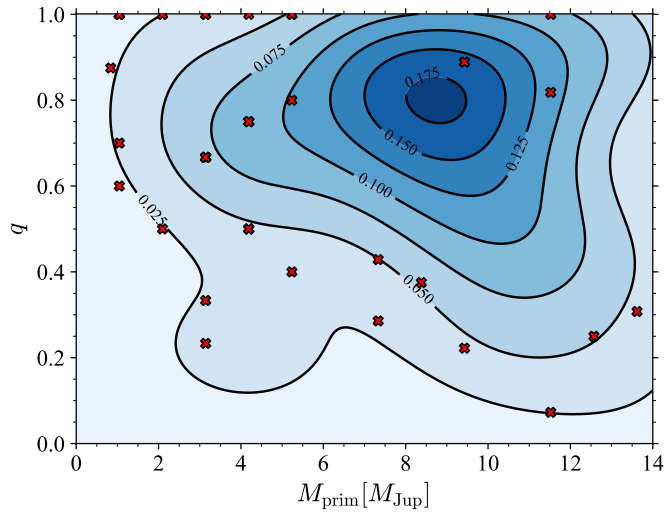

Fig. 14. $M_{\rm prim}$ vs. q contour plot for model F05FFL. Red crosses denote where observed JuMBOs lie.

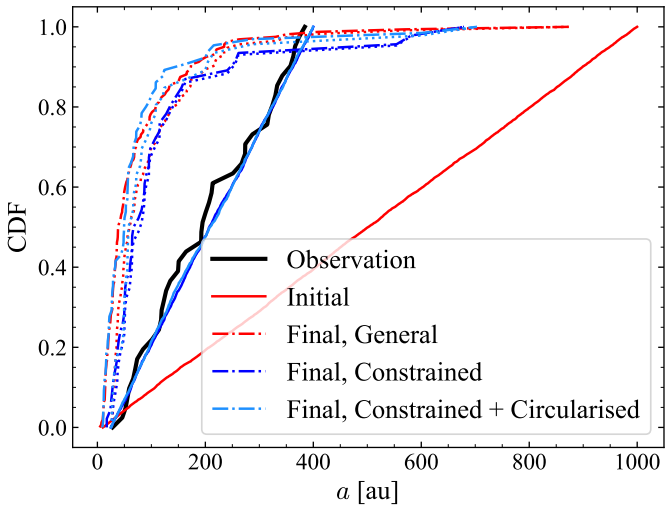

Fig. 15. CDF of surviving JuMBO semi-major axis distribution for models F05, F05O, F05OC.

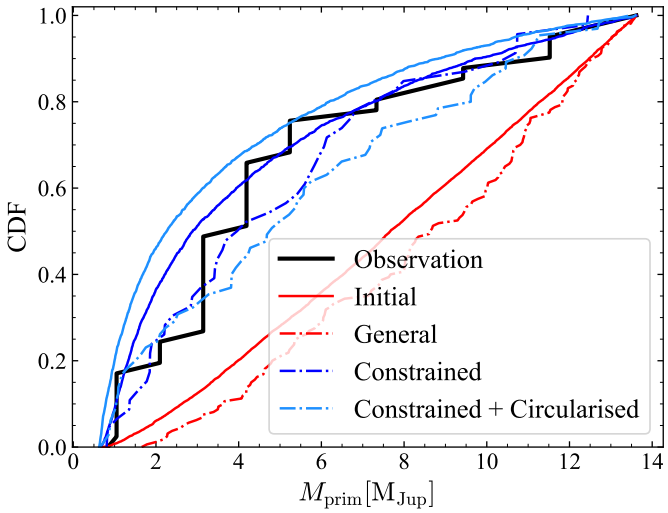

Fig. 16. CDF of surviving JuMBO primary mass for models F05, F05O, F05OC.

7.1.3. Observational Constraints

Our preliminary exploration allows us to rule out Plummer models and further constrain the parameter space. When applying these more restricted initial conditions, $f_{\rm surv}$ and e barely changes while a shows only marginal changes.

This slight increase in $f_{r_{ij}\geq 25\ {\rm au}}$, $\langle a \rangle$ and $\langle r_{ij} \rangle$ could be attributed to the reduction of JMO and JuMBOs present in the environment and the smaller masses they occupy making it harder for them to destabilise wide binaries. The difference in the semi-major axis distribution between models F05, F05O and F05OC (JuMBOs are initially on circular orbits) is shown in figure 15. No matter the configuration, the Fractal models exhibit a natural tendency for trimming out wide binaries.

Figure 16 shows the CDF of primary masses comparing models F05, F05O And F05OC. No matter the configuration, a similar evolution is observed where surviving JuMBOs tend to have larger primary masses. However, unlike the F05 model, the constrained model, initialised with $\alpha = -1.25$, end up being roughly uniform in primary mass compared to the somewhat thermal appearance for F05. In doing, the median primary masses shift towards lower values while the mass ratio towards larger one. A fact reflected by the statistics shown in table 7 and shown in figure 17.

Over the course of our simulation, Fractal runs exhibit a range of dynamical phenomena. The statistics of merging scenarios, and the emergence of both Jupier-mass - Stellar binary systems and $N \geq 3$ systems are summarised in table 8.

Jupiter-mass - stellar mergers could ..... In addition to mergers, ejection events also occured. Though no JuMBOs were ejected, $\sim$ 1 JMO was ejected per simulation and $\sim$ 3 stellar-mass objects.

Figure 18 shows where in (a, e)-space Jupiter-mass - Stellar binaries lie, with little variation between configurations. The parameter space is widely covered, with signs of low-eccentricity but very wide ($a \geq 700$ au) binaries. Nevertheless, the vast majority exhibit large eccentricities and semi-major axis, reflecting their dynamical origin. The non-negligible amount of these systems emerging provide an interesting prospect of detecting ultra-cold Jupiters orbiting stars who have recently fostered them.

Given the poor reproducability in ratios of JuMBOs to JMO free floaters and the tight orbits of JuMBOs we conclude that the

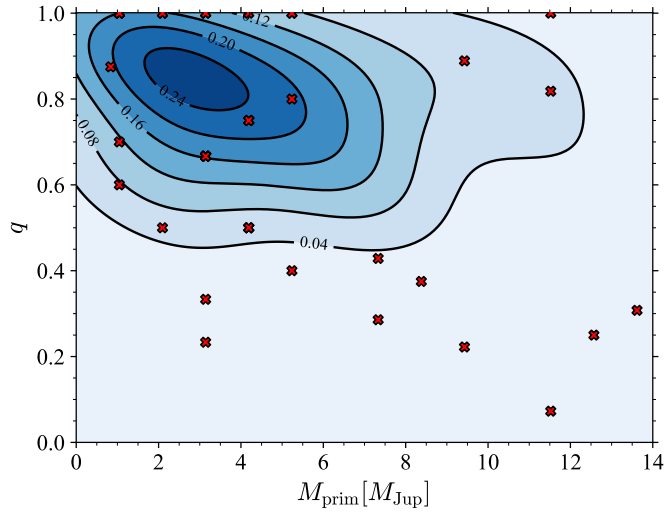

Fig. 17. Contour plot of $M_{\rm prim}$ vs. q for F05O. Red crosses denote where observed JuMBOs lie.

Table 8. TO CHECK

Model	$\langle N_{\rm JS,merge} \rangle$	$\langle N_{\rm SS,merge} \rangle$	$\langle N_{\rm JS} \rangle$	$\langle N_{\rm multi} \rangle$
F05	$2.5^{+0.5}_{-1.5}$	19^{+4}_{-7}	8^{+3}_{-0}	2^{+0}_{-0}
F05FF	$5.5^{+1.5}_{-1.5}$	21^{+2}_{-4}	14^{+1}_{-3}	2^{+0}_{-0}
F1	$1.0^{+1.0}_{-0.0}$	14^{+3}_{-5}	10^{+1}_{-3}	2^{+0}_{-0}
F05FFL	$5.0^{+0.0}_{-1.0}$	22^{+3}_{-5}	$1.0^{+0.0}_{-0.0}$	0^{+7}_{-0}
F05O	$2.0^{+0.8}_{-1.8}$	25^{+2}_{-8}	$4.5^{+2.8}_{-0.5}$	2.0^{+0}_{-0}
F05FFO	$1.0^{+1.0}_{-0.0}$	17^{+3}_{-1}	$5.0^{+1.5}_{-1.0}$	1.0^{+0}_{-0}
F05OC	$0.5^{+2.3}_{-0.5}$	20^{+5}_{-4}	$4.5^{+1.5}_{-1.5}$	3.5^{+0}_{-0}

$\mathcal{ISF}$ models are most likely not the origins of JuMBOs, lending us to our final possible scenario, $\mathcal{FFC}$.

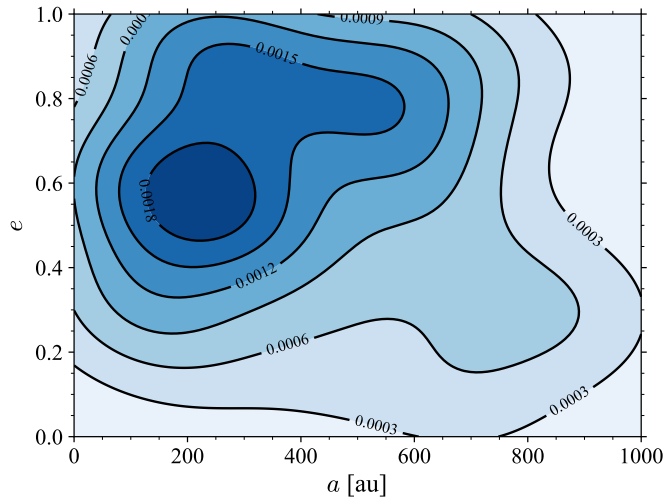

Fig. 18. a vs. e parameter space occupied by Star-JMO binaries during F05FFO runs.

7.2. $\mathcal{FFC}$

8. Discussion

Lorem ipsum dolor sit amet, consectetur adipiscing elit, sed do eiusmod tempor incididunt ut labore et dolore magna aliqua. Ut enim ad minim veniam, quis nostrud exercitation ullamco laboris nisi ut aliquip ex ea commodo consequat. Duis aute irure dolor in reprehenderit in voluptate velit esse cillum dolore eu fugiat nulla pariatur. Excepteur sint occaecat cupidatat non proident, sunt in culpa qui officia deserunt mollit anim id est laborum.

9. Conclusions

9.1. Energy Consumption

The 820 simulations conducted during this investigation had a total wall-clock time of 432 days. For the XYZ runs, each CPU used 6 cores, for the other two configurations 18 cores were used per CPU. In total, the CPU time for all simulations was 7680 days. Assuming a CPU consumption rate of 12 Watt hr^{-1} (**?**), the total energy consumption is roughly 2210 kWh. For an emission intensity of 0.283 kWh kg^{-1} (**?**), our calculations emitted 7.8 tonnes of CO2, roughly equivalent to two round trips by plane New York - Beijing.

Acknowledgements. Veronica Saz Ulibarrena, Shuo Huang, Maite Wilhelm, Brent Maas

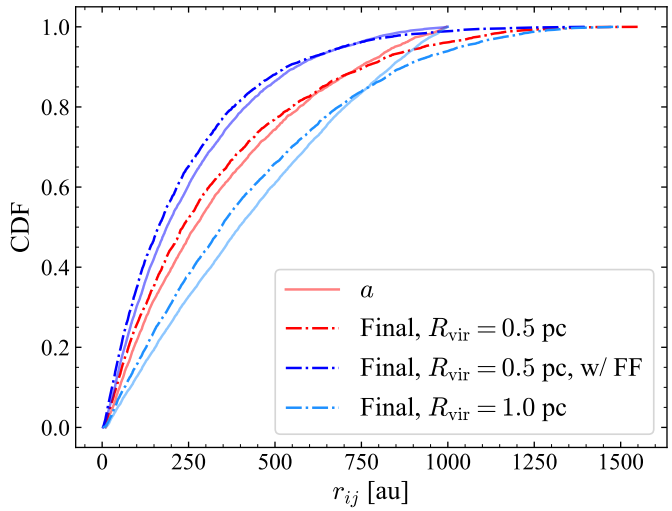

Fig. A.1. CDF of surviving JuMBO projected separation distribution for models P05, P05FF, P1. Overplotted are translucent lines denoting the respective models' JuMBOs semi-major axis.

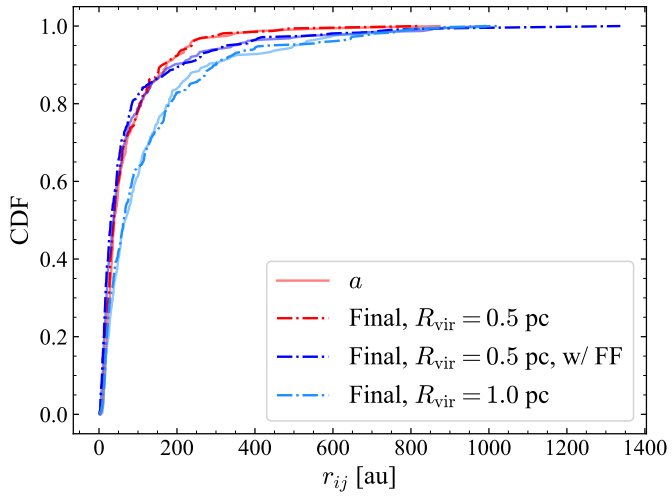

Fig. A.2. CDF of surviving JuMBO projected separation distribution for models F05, F05FF, F1. Overplotted are translucent lines denoting the respective models' JuMBOs semi-major axis.

Appendix A: Similarity between r_{ij} and a

Figures A.1 and A.2 motivate our choice of analysing results in terms of the semi-major axis given the similarity between the curves.

In all cases, r_{ij} exhibits longer tails at the detriment of the shorter separations/orbits. However, these differences are so small - especially in the Fractal case for which most of our discussion revolves around - that we can safely interchange between one and the other. In doing so, we assume that the observed projected separation of JuMBOs are equivalent to their semi-major axis, easing our discussion.

Acknowledgements

Veronica Saz Ulibarrena, Shuo Huang, Maite Wilhelm, Brent Maas, Fred Rasio, Alvaro Hacar.